On the Determination of the Stacking Fault Energy from Extended Nodes in Cu2NiZn

Wegen, G.J.L. van der; Bronsveld, P.M.; Hosson, J.Th.M. De

Published in:
Metallurgical Transactions A

DOI:
10.1007/BF02668136

Publication date:
1980

On the Determination of the Stacking Fault Energy from Extended Nodes in Cu_2NiZn

G. J. L. VAN DER WEGEN, P. M. BRONSVELD, AND J. Th. M. DE HOSSON

Stacking fault energies can be determined from the dimensions of extended dislocation nodes. Different theoretical treatments of the node problem have been published. The aim of the present paper is to compare the results obtained using the theories of Brown and Thölén, Siems and Jøssang *et al* and to provide quantitative information about the dependence of the stacking fault energy for Cu_2NiZn on the model used. Extended nodes in networks with mesh size larger than the outer radius of the node (R) can be used for the determination of the stacking fault energy. Isolated nodes as well as network nodes are used to obtain the stacking fault energy in Cu_2NiZn, which appeared to be 33 ± 9 mJ/m^2.

IT has been well established that $\frac{1}{2}\langle 110\rangle$ dislocations in some fcc metals and alloys dissociate into Shockley partials on the $\{111\}$ slip plane. The separation of the two partials is determined by the stacking fault energy. The lower the stacking fault energy, the wider the split and the more rigorously should slip be confined to a $\{111\}$ slip plane.

The stacking fault energy γ has been shown to be the principal factor determining the unidirectional work-hardening behavior of various fcc metals and alloys. More precisely, the dimensionless parameter γ/Gb, where G is the shear modulus and b the slip distance, gives a measure of the ease of cross slip of screw dislocations and hence determines the work-hardening behavior. The stacking fault energy γ is therefore a property of great physical importance; unfortunately it is also difficult to measure accurately.

There has been considerable controversy over the correct values of γ for various fcc metals and alloys. At various times different authors have cited values differing by a factor of 4 for the same metal. For Cu after twenty years during which γ was estimated to be as low as 24 mJ/m^2 (Ref. 1) and as high as 163 mJ/m^2 (Ref. 2), the measurement by Cockayne *et al*[3] ($\gamma = 41 \pm 9$ mJ/m^2) results in a value very close to the original estimate of Fullman.[4] Although the subject is still controversial, it is generally believed that the node method originated by Whelan[5] and improved by others[6,7] provides reliable values for the stacking fault energy. However, especially in the case of Cu the nodes are small and the node method is difficult to apply to some extent of accuracy.

By transmission electron microscopy we have already characterized superlattice dislocations in Cu_2NiZn.[8] The superlattice dislocation in an ordered crystal consists essentially of two ordinary dislocations ($b = \frac{1}{2}\langle 110\rangle$) joined by an antiphase boundary. In fcc crystal structures, however, the superlattice dislocation is complicated by the splitting of each of these dislocations into Shockley partials on a $\{111\}$ plane. If the slip system is known, the separations between the partials of a superlattice dislocation can be calculated within the framework of anisotropic elasticity theory using values for the ordering energy and the stacking fault energy.[9] Inversely, measuring the separations between the partials will produce values for the interaction energies between the different species and for the stacking fault energy which all determine the mechanical properties. However, the partials of two unit dislocations could not be detected with magnification up to 93,000 times from which we may conclude that it is obviously impossible, using the Philips EM 300, to obtain a reliable value for the stacking fault energy in Cu_2NiZn, assuming that the antiphase boundary energies are known.

Nevertheless, based on the work of Swann and Nutting[10] on Cu_3Zn, it may be expected that in the alloy Cu_2NiZn lower values of the stacking fault energy may be obtained than in the constituent pure metals. For this reason, we have applied the method utilizing extended dislocation nodes in order to obtain a reliable value of γ. One should keep in mind though, that both dislocation locking and ordering can complicate and sometimes obscure the effects of having varied the stacking fault energy on alloying. Different theoretical treatments of the node problem have been published in the literature. In particular we will focus our attention on three different theoretical analyses based on the theory of Brown and Thölén,[11] of Siems[12] and of Jøssang *et al*.[7] For a comprehensive survey of those treatments reference should be made to Ruff.[13] The aim of the present paper is to compare the results obtained using different treatments and to provide quantitative information about the actual sensitivity of stacking fault energy for Cu_2NiZn depending on which model has been used.

EXTENDED DISLOCATION NODES

An extended dislocation node is the result of a reaction between two extended dislocations, each of which has its own slip plane and one dislocation is cross slipping into the slip plane of the other.[5]

The three theoretical models as have been mentioned before provide values for the equilibrium configuration of a symmetrical extended node using isotropic elasticity theory. Proceeding on the proposition of a trial shape for an extended node, Brown and Thölén calculated the force due to the faulted stacking, the

G. J. L. VAN DER WEGEN, a Ph.D. Student; P. M. BRONSVELD, a Scientific Co-worker; and J. Th. M. DE HOSSON, Professor of Applied Physics, are all at the University of Groningen, Department of Applied Physics, Materials Science Centre, Nijenborgh 18, 9747 AG Groningen, The Netherlands.

Manuscript submitted November 8, 1979.

dislocation interactions between the other nodal dislocations and the normal force on the dislocation line due to the self stress of the dislocation. This is done at forty-one points along a bounding partial dislocation. Each point is displaced proportionally to the stress exerted. The force at each point is recalculated. This iterative procedure is halted when the total force at each point has vanished, determining the equilibrium shape of the node. The results of the calculations are summarized in two equations:

$$\frac{\gamma R}{G\mathbf{b}_p^2} = 0.27 - 0.08\left(\frac{\nu}{1-\nu}\right)\cos 2\alpha + \left\{0.104\left(\frac{2-\nu}{1-\nu}\right) + 0.24\left(\frac{\nu}{1-\nu}\right)\cos 2\alpha\right\}\log_{10}\frac{R}{\epsilon}, \quad [1]$$

$$\frac{\gamma y}{G\mathbf{b}_p^2} = 0.055\left(\frac{2-\nu}{1-\nu}\right) - 0.06\left(\frac{\nu}{(1-\nu)^2}\right)\cos 2\alpha + \left\{0.018\left(\frac{2-\nu}{1-\nu}\right) + 0.036\left(\frac{\nu}{1-\nu}\right)\cos 2\alpha\right\}\log_{10}\frac{R}{\epsilon}, \quad [2]$$

where γ is the stacking fault energy, $\mathbf{b}_p$ is the length of the Burgers vector of the partial dislocation, G is the shear modulus, ν is Poisson's ratio, α is the character of the node, ϵ is a cut-off parameter ($\epsilon = \mathbf{b}_p$ should be an appropriate choice[11]), R is the outer radius and y the inner radius of the extended node (Fig. 1). The coefficients have been chosen to fit the computed values within an accuracy of 10 pct.

Siems determines the configuration of minimum total energy using Lagrange's method of undetermined multipliers. As total energy he also sums the stacking fault energy, the interaction energy between the nodal dislocations and the line energy. The variation of the line energy with character α of the partial dislocation has been taken into account. However, the theory considers the interaction energy between two partials of one branch of the extended node and approximates the interaction energy assuming two parallel dislocation lines. This theory yields the following equations:

$$\frac{\gamma R}{G\mathbf{b}_p^2} = \frac{1}{4\pi}\left(\frac{Q_0}{Q_0-1}\right)\left[1 + \frac{\nu(1+3\cos 2\alpha}{2(1-\nu)}\right]\log_e\frac{R}{\epsilon}, \quad [3]$$

$$\frac{\gamma y}{G\mathbf{b}_p^2} = \frac{Q_0}{8\sqrt{3}\pi}\left[\frac{2-\nu(1+2\cos 2\alpha)}{(1-\nu)}\right], \quad [4]$$

where Q_0 is a parameter satisfying the equation:

$$Q_0 - 1 - \log_e Q_0 = \left(\frac{\sqrt{3}-1}{2}\right)\left[\frac{\sqrt{3}(2-\nu)}{2-\nu(1+2\cos 2\alpha)} - 1\right]\log_e\frac{R}{\epsilon}, \quad [5]$$

being proportional to the relative fault width expansion at the extended node center:

$$Q_0 = \sqrt{3}(y/d), \quad [6]$$

where

$$d = \frac{G\mathbf{b}_p^2}{8\pi\gamma}\left(\frac{2-\nu}{1-\nu}\right)\left(1 - \left(\frac{2\nu}{2-\nu}\right)\cos 2\alpha\right) \quad [7]$$

represents the separation of the partials forming a node arm at large distance from the node center (Fig. 1). The same value for the cut-off parameter ϵ should be applied as in the theory of Brown and Thölén.

The theory of Jøssang *et al* calculates the exact energy of an angular dislocation configuration that approximates the shape of the extended node (Fig. 2). The double angular dislocation configuration has the same stacking fault area as the actual node. The energy difference between the angular configuration and the actual one is very small. For a discussion the reader is referred to the original paper.[7] Based on this model values of Σ_0 as a function of β are obtained, using the following expressions:

$$\Sigma_0 = \frac{8\pi\sqrt{3}(1-\nu)\gamma Z_0}{G\mathbf{b}_p^2\{2-\nu(1+2\cos 2\alpha)\}} = \sqrt{3}\left(\frac{Z_0}{d}\right) \quad [8]$$

and

$$\beta = \frac{\gamma}{p\mathbf{b}_p G}, \quad [9]$$

where $p = \mathbf{b}_p/2\epsilon$ and Z_0 is empirically in the range $1.10y$ to $1.15y$. Comparison of the three theories shows that

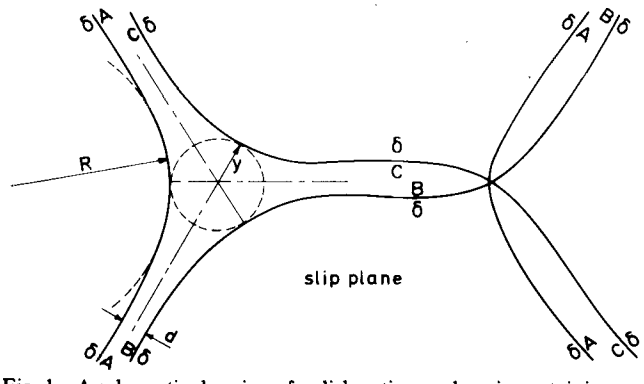

Fig. 1—A schematic drawing of a dislocation node pair containing intrinsic stacking faults. Burgers vector of the partials are indicated in Thompson's notation.

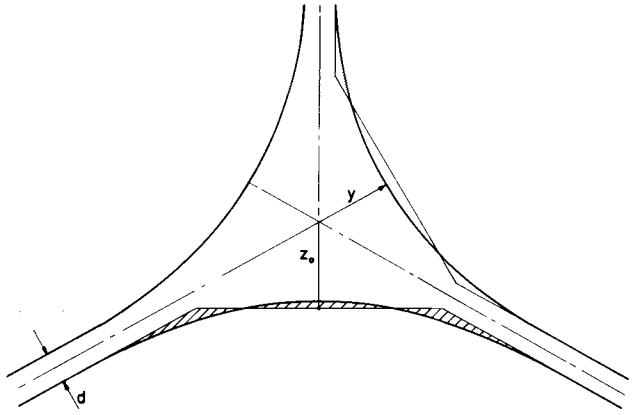

Fig. 2—Double angular dislocation configuration approximating the node configuration in the theory of Jøssang *et al.*

for screw ($\alpha = 0°$) extended nodes all three theories result into almost the same values for the stacking fault energy (when $p = 2$ is taken in Jøssang's theory). There exists a large difference for edge-oriented ($\alpha = 90°$) extended nodes. Measuring the stacking fault energy from nodes of edge type, therefore will provide a critical test on the different models. Unfortunately, only a few extended nodes with $\alpha > 50°$ are observed.

ELECTRON IMAGING AND MEASUREMENT

Extended nodes in fcc materials consist of an intrinsic stacking fault, with fault vector **R** of type $\frac{1}{6}a_0\langle 211\rangle$, bounded by Shockley partials with Burgers vector of type $\frac{1}{6}a_0\langle 211\rangle$, lying in slip planes of type {111} (Fig. 1). The Burgers vector of a dislocation can be determined by using the criterion that the dislocation is invisible if $\mathbf{g} \cdot \mathbf{b} = 0$ and $\mathbf{g} \cdot \mathbf{b} \wedge \mathbf{u}$ is sufficiently small ($\lesssim 0.5$),[14] where **g** is the diffraction vector, **b** is the Burgers vector and **u** represents the unit vector along the dislocation line. The slip plane can be determined by tilting experiments. The character of each arm of the node is described by the angle between the line direction of the arm and the total Burgers vector of the arm. If all three arms of the node have the same character, the node is called character-symmetric. Diffraction vectors used for identification of the Shockley partials are of type $\langle 220\rangle$ and $\langle 111\rangle$. The diffraction vectors are listed in Table I.

One should keep in mind that partials imaged with $\mathbf{g} \cdot \mathbf{b} = \pm\frac{1}{3}$ are effectively invisible.[15] Stacking fault contrast occurs when $\alpha = 2\pi\mathbf{g} \cdot \mathbf{R} \neq 2\pi n$, where n is an integer. Because the normal on the stacking fault plane (identical to slip plane) makes an angle with the foil normal, stacking fault fringes are visible in Fig. 3(*b*). The fringes run parallel with the secant of the stacking fault plane and the surface of the foil. Almost all grains have a [110] orientation near the foil normal, due to rolling texture. Only (111) and $(11\bar{1})$ slip planes can be oriented perpendicular to the beam due to the limiting tilt angle. Therefore, as a result the fringes of extended nodes in these two slip planes have a $[1\bar{1}0]$ direction.

The nodes are imaged in the dark field weak-beam mode.[16] This technique is an effective method for measuring extended node dimensions since the position of the dislocation image is less than 0.7 nm apart from the dislocation core position under condition that $|s_g| \geq 0.2\ \mathrm{nm}^{-1}$ and $|w| = |\xi_g \cdot s_g| \geq 5$ is fulfilled.[14] Here, s_g is the deviation parameter from exact Bragg position and ξ_g is the extinction distance (both associated with the reflection used for the image). Since the image of the partials of an extended node lie on the same side of the cores, the measured dimensions of the extended node differ less than 0.7 nm from the actual dimensions, using the above values of $|s_g|$ and $|w|$. The nodes are imaged in two different ways to measure the separations: in dislocation line contrast using a diffraction vector of type $\langle 113\rangle$, when the grain is in a $\langle 211\rangle$ orientation (Fig. 3(*a*)) and in stacking fault contrast using a diffraction vector of type $\langle 111\rangle$, when the grain is in a $\langle 211\rangle$ orientation (Fig. 3(*b*)). Contrast of the first type exhibits also a weak stacking fault contrast.

The nodes are imaged in the electron microscope at a magnification of about 75,000 times. Further photographic enlargement produces the final picture for measurements. The measuring technique applied here consists of superimposing a series of circular annuli, choosing the ones which best fit to the inner and outer radii of the extended node. Because the projection plane (type {211}) makes a small angle with the slip plane (type {111}) one has to contend with a small geometric distortion of the extended node in the projection plane. For symmetric extended nodes, Ruff[13] provides a formula for separate corrections on the three different inner radii and takes the average value. Because the dimensions of the extended nodes measured in Cu_2NiZn are very small another correcting procedure is applied using Table XII of Ref. 13. The average of the correction factors corresponding to the angle ψ (= angle between projection plane and slip plane) is used to

Table I. g · b and g · R Values for ⟨220⟩ and ⟨111⟩ Reflections

b\g	$[2\bar{2}0]$	$[20\bar{2}]$	$[02\bar{2}]$	$[\bar{1}11]$	$[1\bar{1}1]$	$[11\bar{1}]$
$\frac{1}{6}[\bar{2}11]$	−1	−1	0	+2/3	−1/3	−1/3
$\frac{1}{6}[1\bar{2}1]$	+1	0	−1	−1/3	+2/3	−1/3
$\frac{1}{6}[11\bar{2}]$	0	+1	+1	−1/3	−1/3	+2/3
$\mathbf{R} = \frac{1}{6}\langle 11\bar{2}\rangle$	0	+1	+1	−1/3	−1/3	+2/3

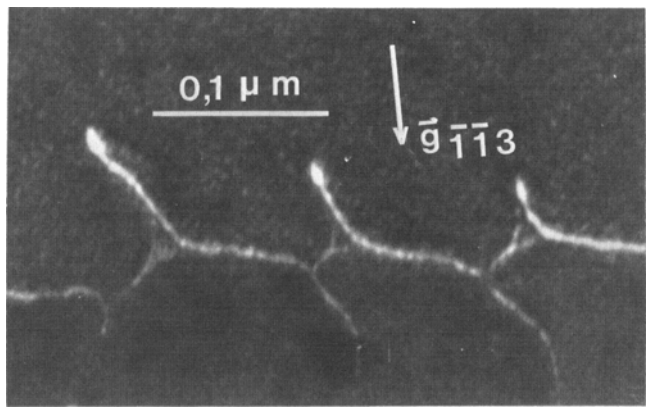

(a)

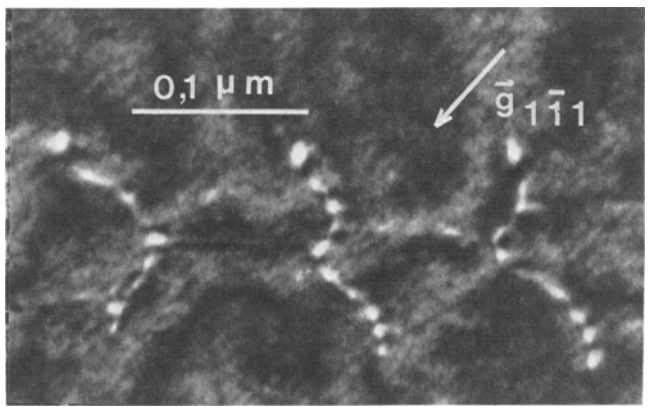

(b)

Fig. 3—(*a*) Three dislocation node pairs of screw type imaged in dislocation line contrast. Dark field weak-beam image; projection plane (211); $\mathbf{g} = [\bar{1}\bar{1}3]$; $s_g = 0.15\ (\mathrm{nm}^{-1})$; $\alpha = 60$ deg; (111) slip plane. (*b*) Same nodes as Fig. 3(*a*) imaged in stacking fault contrast. Dark field weak-beam image; (121) projection plane; $\mathbf{g} = [1\bar{1}1]$; $s_g = 0.10\ (\mathrm{nm}^{-1})$.

correct the circle chosen by the criterion as mentioned above. The latter is actually an averaging technique which minimizes the geometric distortion. This procedure should provide the radii with an accuracy of 1 pct. Isolated and symmetrical nodes, at large distance from foil surfaces and grain boundaries, will produce the most reliable results for the stacking fault energy. Most extended nodes appear in networks but they can still be utilized, provided that the network mesh size is larger than the outer radius of the extended node, which is the case in the network shown in Fig. 3.

The foils have been prepared in the same way as in Ref. 8. The sample is annealed at 838 K for 10 min, having a composition of 51 at. pct Cu, 25 at. pct Ni and 24 at. pct Zn.

RESULTS

In the Cu_2NiZn alloy deformed 5 pct in tension, two isolated extended nodes and a network of thirteen extended nodes are characterized using the method described in the previous section. It appeared that all nodes in the network are of the same character. The network is probably formed by the intersection of an extended ordinary dislocation with a dislocation pile-up. Since all dislocations in a pile-up have the same Burgers vector and the same dislocation line direction (*i.e.* they have the same character), it is to be expected that also all nodes of the network have the same character. The network consists of 60 deg nodes and both isolated nodes are 30 deg in character.

From neutron diffraction experiments[17] on Cu_2NiZn at room temperature, a lattice parameter $a_0 = 0.36380 \pm 0.00004$ nm is obtained and this value is used in the calculation of $\mathbf{b}_p$. Values of the elastic constants (C_{ij}) for the alloy Cu_2NiZn are obtained theoretically by J. de Groot *et al.*[9] Their values are: $C_{11} = 1.635 \times 10^{11}$ N/m^2, $C_{12} = 1.185 \times 10^{11}$ N/m^2 and $C_{44} = 0.836 \times 10^{11}$ N/m^2. For cubic materials Teutonico[18] found good agreement between the width of extended dislocations calculated from anisotropic theory with those obtained from isotropic theory using the effective values of G and ν for glide on {111} planes. Using these values of the elastic constants it is found that $G_{\text{eff}} = 4.34 \times 10^{10}$ N/m^2 and $\nu_{\text{eff}} = 0.446$. With these effective values of G and ν curves of $\gamma R/G\mathbf{b}_p^2$ and $\gamma y/G\mathbf{b}_p^2$ are drawn as a function of R for several α-values according to the theory of Brown and Thölén (Fig. 4) and according to the theory of Siems (Fig. 5). In Fig. 6 Σ_0 is plotted as a function of β for several α-values according to the theory of Jøssang *et al.* From these curves the stacking fault energy is determined using the measured quantities y and R. The results are compiled in Table II.

Table II. Measured Radii and Calculated Stacking Fault Energies

α	y	R	$\gamma(y)$	$\gamma(R)$	$\gamma(y)$	$\gamma(R)$	$\gamma(y)$ $p = 2$	$\gamma(y)$ $p = \frac{1}{2}$
	(nm)	(nm)	Siems		$B + T$		Jøssang	
60°	6.5	36.2	32	18	41	24[5]	34	31
30°	8.4	29.9	29	33	30	36[5]	28	24[5]
30°	6.4	33.3	36[5]	30	38	33	36[5]	32
average			33	27	36[5]	31	33	29

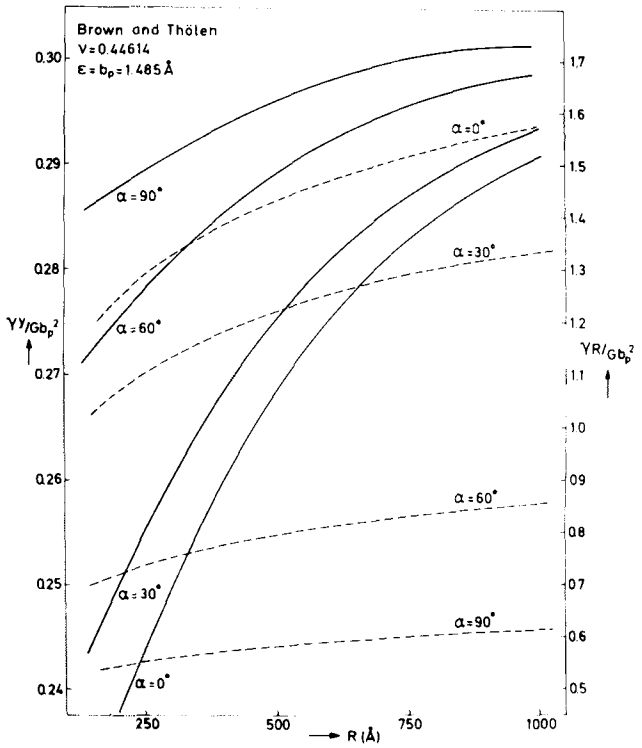

Fig. 4—$\gamma R/G\mathbf{b}_p^2$-values (-----) and $\gamma y/G\mathbf{b}_p^2$-values (——) as a function of R for several α values according to the theory of Brown and Thölén.

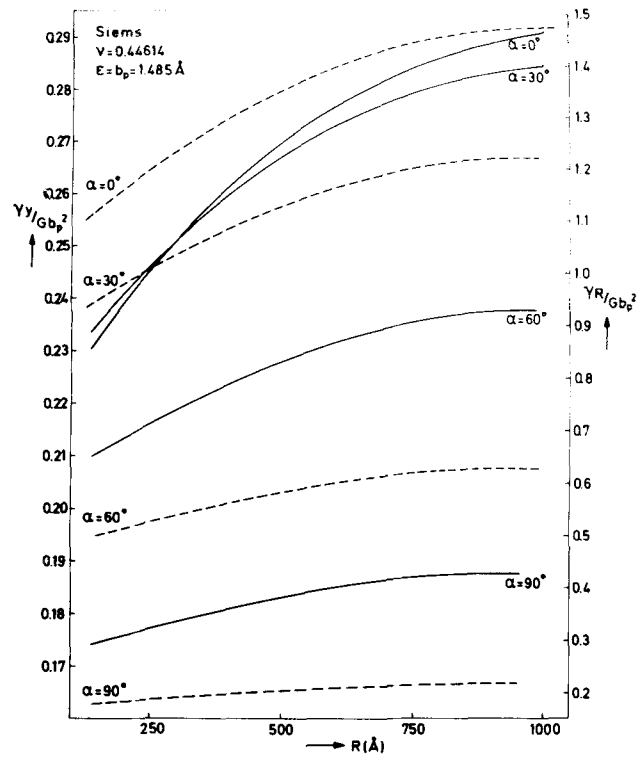

Fig. 5—$\gamma R/G\mathbf{b}_p^2$-values (-----) and $\gamma y/G\mathbf{b}_p^2$-values (——) as a function of R for several α values according to the theory of Siems.

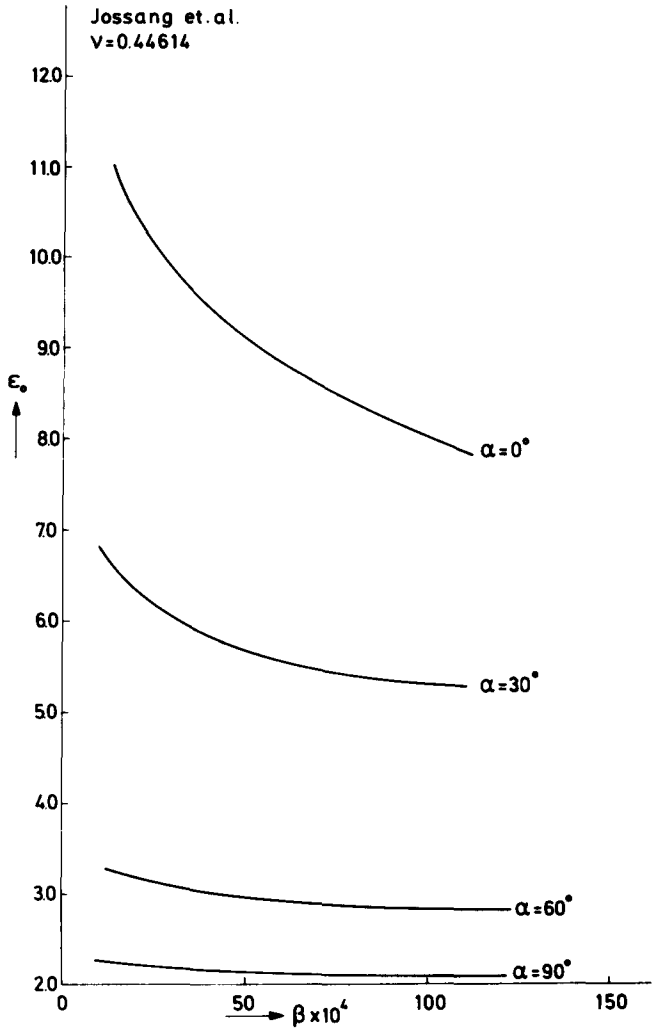

Fig. 6—Σ_0 as a function of β for several α values according to the theory of Jøssang *et al.*

DISCUSSION

Determination of the stacking fault energy on extended nodes has to be done with utmost care. Considerable errors can be introduced by a non-equilibrium shape of the extended nodes or by imaging effects. Inhomogeneities in composition are minimized by an annealing treatment at 1123 K for four days. Internal stresses due to dislocation interactions, free surfaces and grain boundary effects are minimized by taking nodes which are at large distances from other dislocations and surfaces (*e.g.* isolated nodes). However, Ruff[13] suggested that a network of nodes can be used if the network mesh size is larger than R (outer radius of the node). Since this is the case in the observed network, values for the stacking fault energy are also determined from these extended nodes. The assumption seems to be justified because the average value of the stacking fault energy calculated from the network of extended nodes is not different from the value obtained from two isolated extended nodes (Table II). Important quantities in imaging are the magnification and the position of the image intensity peak of a dislocation with respect to its core position. The error in the magnification is less than 2 pct when the overall magnification is calibrated, keeping the objective lens current at the same value, which is applied during the imaging of an extended node. As mentioned before the imaged separation of the nodal partials does not differ more than about 0.7 nm from the actual separation of the cores, using the indicated values of $|s_g|$ and $|w|$.

Other errors can be introduced by measuring the inner and outer radii of the imaged extended nodes. As the inner radius is very small there is an appreciable error in its measurement of about 3 pct. However, being extremely careful, it should be possible to determine the node dimensions within a 10 pct overall accuracy.

By a rapid quench from the annealing temperature of 838 K (above the critical temperature for long range order $T_c \approx 768$ K) the disordered state is quenched in. In the electron microscope the specimen is heated by the electron beam, which can initiate ordering. As a result the extended nodes may decrease in size as the internal energy of the faulted area is increased by ordering. This leads to an overestimate of the stacking fault energy. However, since no superlattice reflections could be detected long range order did not exist. In summary we can state that the stacking fault energy of Cu_2NiZn is 33 ± 9 mJ/m^2. This value is obtained from Table II. Arguing from the values of the stacking fault energies in pure Cu and pure Ni, it could be expected that on alloying stacking fault energies will be in the range 41 to 120 mJ/m^2. Halder *et al*[19] found that the influence of the Ni content on the latter is small in ternary CuNiZn alloys. Addition of Zn (hexagonal structure) decreases the stacking fault energy,[19] because the stacking fault area has a hexagonal configuration. Based on the above consideration, a stacking fault energy of Cu_2NiZn close to that of pure Cu, as found in our experiments, is not surprising.

CONCLUSIONS

From this work the following conclusions can be stated:

1. Extended nodes have not been observed in polycrystalline specimens deformed one or three pct in tension. A dislocation density corresponding to a deformation of about five pct is required for the formation of extended nodes in Cu_2NiZn. They appear as part of a network as well as isolated.
2. The weak-beam method for determination of the stacking fault energy from extended nodes is readily applied to a Cu_2NiZn alloy.
3. The stacking fault energy of Cu_2NiZn determined in this work is 33 ± 9 mJ/m^2.
4. The stacking fault energy determined by a measurement of the outer radius of the extended node yields in most cases a smaller value than the one obtained from the inner radius. The latter is more reliable because the fitting of the circular annuli within the node is more consistent.
5. Extended nodes in a network with mesh size larger than R yields a value for the stacking fault energy that does not differ from those obtained from isolated nodes.
6. A good theory should predict a stacking fault energy independent of the node character α, therefore

the value of $\gamma(y)$ (which is more reliable than $\gamma(R)$) for the 60 deg node should be equal to the average value of $\gamma(y)$ for the two 30 deg nodes within each theory. A comparison of values from Table II shows that the largest deviation occurs for the theory of Brown and Thölén.

However, because the scatter of the values of the 30 deg nodes within each theory is rather large, one might choose for an alternative approach by starting from the average value of one 30 deg node over the three theories and comparing the individual 60 deg node with this average value. The first 30 deg extended node yields an average value of about 28 mJ/m^2, supporting Siems' theory and Jøssang's theory with $p = \frac{1}{2}$ which results in a value of 32 and 31 mJ/m^2, respectively, for the 60 deg extended nodes. The second 30 deg extended node yields an average value of about 36 mJ/m^2, supporting the theory of Brown and Thölén and Jøssang's theory with $p = 2$ which results in a value of 41 and 34 mJ/m^2, respectively, for the 60 deg extended nodes.

7. The difference between the three theories is clearly shown in the values for the stacking fault energy of Table II. Determination of the stacking fault energy of Cu_2NiZn using other methods (for instance: faulted dipoles or multiple ribbons) could result in a preference for one of the three theories.

ACKNOWLEDGMENTS

Particular thanks are due to Mr. H. J. Bron and Mr. U. B. Nieborg for technical assistance in preparing the samples. The work reported was carried out as part of a project on ordering in ternary alloys of the Foundation for Fundamental Research on Matter (F.O.M.–Mt VI-2) at Utrecht and was also made possible by financial support from the Netherlands Organization for the Advancement of Pure Research (Z.W.O.) at the Hague.

REFERENCES

1. M. C. Inman and A. R. Kahn: *Philos. Mag.*, 1961, vol. 6, p. 937.
2. A. Seeger, R. Berner, and H. Wolf: *Z. Phil.*, 1959, vol. 155, p. 247.
3. D. J. H. Cockayne, M. L. Jenkins, and I. L. F. Ray: *Philos. Mag.*, 1971, vol. 24, p. 1383.
4. R. Fullman: *J. Appl. Phys.*, 1951, vol. 22, p. 448.
5. M. J. Whelan: *Proc. Roy. Soc. A*, 1959, vol. 249, p. 114.
6. L. M. Brown: *Philos. Mag.*, 1964, vol. 10, p. 441.
7. T. Jøssang, M. J. Stowell, J. P. Hirth, and J. Lothe: *Acta Metall.*, 1965, vol. 13, p. 279.
8. G. J. L. van der Wegen, P. M. Bronsveld, and J. Th. M. de Hosson: *Scr. Metall.*, 1979, vol. 13, p. 303.
9. J. de Groot, P. M. Bronsveld, and J. Th. M. de Hosson: *Phys. Status Solidi (A)*, 1979, vol. 52, p. 635.
10. P. R. Swann and J. Nutting: *J. Inst. Met.*, 1961, vol. 90, p. 133.
11. L. M. Brown and A. R. Thölén: *Discuss. Faraday Soc.*, 1964, vol. 38, p. 35.
12. R. Siems: *Discuss. Faraday Soc.*, 1964, vol. 38, p. 42.
13. A. W. Ruff: *Met. Trans.*, 1970, vol. 1, p. 2391.
14. D. J. H. Cockayne: *Z. Naturforsch.*, 1972, vol. 27a, p. 452.
15. A. Howie and M. J. Whelan: *Proc. Roy. Soc. A*, 1962, vol. 267, p. 206.
16. D. J. H. Cockayne, I. L. F. Ray, and M. J. Whelan: *Philos. Mag.*, 1969, vol. 20, p. 1265.
17. J. Vrijen, P. M. Bronsveld, J. van der Veen, and S. Radelaar: *Z. Metallkd.*, 1976, vol. 67, p. 473.
18. L. J. Teutonico: *Philos. Mag.*, 1967, vol. 15, p. 959.
19. S. K. Halder, M. De, and S. P. Sen Gupta: *J. Appl. Phys.*, 1977, vol. 48, p. 3560.